

AD-A040 192

CATHOLIC UNIV OF AMERICA WASHINGTON D C VITREOUS STA--ETC F/G 11/2  
SUMMARY OF RESEARCH ON STRUCTURAL RELAXATION, ELECTRICAL RELAXA--ETC(U)  
MAR 77 T A LITOVITZ, P B MACEDO, C T MOYNIHAN AF-AFOSR-2203-72  
AFOSR-TR-77-0648 NL

UNCLASSIFIED

| OF |

AD  
A040 192



END

DATE  
FILMED

6-77

APR 8 REC'D

SUMMARY OF RESEARCH ON STRUCTURAL RELAXATION,  
ELECTRICAL RELAXATION, PHASE SEPARATION AND  
MICROSTRUCTURE IN GLASSES

12

Final Report

Contract No. AFOSR 72-2203

Sponsored by Air Force Office of Scientific Research

Bolling Air Force Base

Washington, DC 20332

by

Vitreous State Laboratory

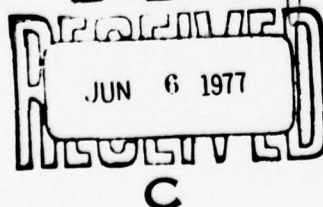
Catholic University of America

Washington, DC 20064

March 31, 1977

Reproduction in whole or in part is permitted for any  
purpose of the United States Government.

AD No. 1  
DDC FILE COPY



Approved for public release  
Distribution unlimited.

1473 in rear →

ADA040192

AIR FORCE OFFICE OF SCIENTIFIC RESEARCH (AFSC)  
NOTICE OF TRANSMITTAL TO DDC  
This technical report has been reviewed and is  
approved for public release IAW AFR 190-12 (7b).  
Distribution is unlimited.  
A. D. BLOSE  
Technical Information Officer

DDC LIFE COB  
DDC HQ

AFR 77-1100

REPORT DOCUMENTATION PAGE		READ INSTRUCTIONS BEFORE COMPLETING FORM
1. REPORT NUMBER AFOSR - TR - 77 - 0648	2. GOVT ACCESSION NO.	3. RECIPIENT'S CATALOG NUMBER
4. TITLE (and Subtitle) SUMMARY OF RESEARCH ON STRUCTURAL RELAXATION, ELECTRICAL RELAXATION, PHASE SEPARATION AND MICROSTRUCTURE IN GLASSES.		5. TYPE OF REPORT & PERIOD COVERED Final, 1 Sep 71 - 31 Aug 76
6. AUTHOR(s) T.A./Litovitz, P.B./Macedo, C.T./Moynihan, P.K./Gupta, J.H./Simmons		7. PERFORMING ORG. REPORT NUMBER
9. PERFORMING ORGANIZATION NAME AND ADDRESS Vitreous State Laboratory Catholic University of America Washington, DC 20064		8. CONTRACT OR GRANT NUMBER(s) AFOSR 72-2203 13 AF-AFOSR-2203-77
11. CONTROLLING OFFICE NAME AND ADDRESS AF Office of Scientific Research/NC Bolling AFB, DC 20332		10. PROGRAM ELEMENT, PROJECT, TASK AREA & WORK UNIT NUMBERS 2303/A3, 61102F
14. MONITORING AGENCY NAME & ADDRESS (if different from Controlling Office)		12. REPORT DATE 31 Mar 77 12-41p
		15. SECURITY CLASS. (of this report) Unclassified
16. DISTRIBUTION STATEMENT (of this Report)  Approved for public release; distribution unlimited.		15a. DECLASSIFICATION/DOWNGRADING SCHEDULE
17. DISTRIBUTION STATEMENT (of the abstract entered in Block 20, if different from Report) 18 AFOSR 19 TR-77-0648		
18. SUPPLEMENTARY NOTES 16-2303 17-A3		
19. KEY WORDS (Continue on reverse side if necessary and identify by block number)		
20. ABSTRACT (Continue on reverse side if necessary and identify by block number) The study of glasses and glass-forming liquids (vitreous materials) constituted an area of basic research in chemistry rich in immediate applications to technology of importance to the Air Force. The fundamental output of this contract has been 18 basic scientific publications in the general areas of 1) micro-structure and phase separation, 2) electrical relaxation phenomena and 3) viscoelastic and structural relaxation in molten glasses. 404 951-SS		



## I. INTRODUCTION

In 1971 the Vitreous State Laboratory of the Catholic University of America proposed to the Air Force Office of Scientific Research a program of research on the optical, infra-red and mechanical properties of glass. We stated that the study of glasses and glass-forming liquids (vitreous materials) constituted an area of basic research in chemistry rich in immediate applications to technology of importance to the Air Force.

Our premise was that we were proposing to do valid, state-of-the-art basic research, but in areas where the probability of impacting defense technology was high. We submit that that premise of five years ago proved to be a reality beyond even our highest expectations.

The fundamental output of this contract has been 18 basic scientific publications in the general areas of 1) micro-structure and phase separation, 2) electrical relaxation phenomena and 3) viscoelastic and structural relaxation in molten glasses. The contributions of these publications to basic knowledge in their respective areas are summarized in Sections III-V. Before becoming involved with the details of this basic work, however, we describe briefly in the following section the impact of this work in three applied areas of current technological importance to the defense establishment.

ACCESSION FOR	
NTIS	White Section
DOB	Ref Section
UNANNOUNCED	
JUSTIFICATION	
BY	
DISTRIBUTION/AVAILABILITY CODE	
Dist.	AVAIL. AND/OR SPECIF.

## II. RELEVANCE TO TECHNOLOGICAL PROBLEMS

### A. Fiber Optics Technology

We have produced on this contract a series of basic papers on liquid/liquid phase separation. Our research into isolating the earliest states of phase separation made us familiar with every facet of this process. Out of this work we discovered (invented) an entirely new approach to the purification of glass for the manufacture of fiber optic waveguides. This new technology will allow production of fibers from relatively impure starting materials (e.g., sand). The cost today of low loss fiber optic cable is about \$1,000 per km, so that our technique may yield a savings of tens of millions of dollars on future DOD procurement costs.

Not only will there be a cost reduction. Out of the above research also came the concept of making very strong fibers by doping leached, phase separated preforms with dopants specifically chosen to introduce compressional stresses at the surface of the preform. This approach, now supported by Air Force Cambridge Research Laboratories, promises to combine low cost and high strength, making possible many DOD uses not previously feasible.

In addition to the advantages mentioned above, recent preliminary evidence indicates that the above fiber gives unexpectedly good performance following exposure to radiation.

## B. Radar Dome Technology

Our basic research in phase separation and electrical conduction has allowed us to produce a material that has a strength comparable to the glass ceramics now being used for radomes, but which has significantly higher laser radiation resistance and much lower (by orders of magnitude) electrical conductance. This latter feature makes it more transparent to radar waves even at high temperatures where the present radar domes fail.

## C. Lubrication Technology

From our basic research on structural and viscoelastic relaxation in the glass melts we developed techniques to measure and analyze linear viscoelastic behavior using light scattering methods and non-linear behavior using differential scanning calorimetry and dilatometry. This led to a new theoretical approach for the calculation of viscoelastic properties following any type of thermal history. This has led to the development of a new theory for the prediction of the behavior of lubricants in a contact. This new theory which predicts that a liquid lubricant behaves as a glass in the contact zone should have a considerable impact on the design of new synthetic lubricants.

In summary, the research dollars AFOSR spent at Catholic University over the past years should be returned many times over in cost savings, in addition to improving materials performance in many areas.

### III. STRUCTURAL RELAXATION AND VISCOELASTICITY

When a liquid is subjected to a rapid change in temperature, pressure, or stress, it exhibits an instantaneous, solid-like change in properties such as volume  $V$  and enthalpy  $H$ . This is followed by a slower additional change, due to rearrangement of the liquid structure, of the property until it reaches its equilibrium value at the new temperature, pressure, or stress. This process is illustrated schematically in Fig. 1 for the change in enthalpy  $H$  in response to a temperature step  $\Delta T$ , where  $\Delta H_g$  is the instantaneous, solid-like change in  $H$ , and  $\Delta H_r$  is the change due to the structural relaxation. The response to changes in pressure  $\Delta P$  is of a similar nature.

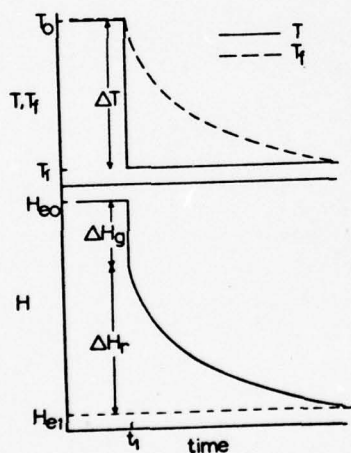


FIGURE 1. Isothermal evolution of enthalpy and fictive temperature following a single temperature step.

It is usually convenient to express the change in the property (e.g.  $H$ ) due to structural relaxation in equivalent temperature units by defining a fictive temperature,  $T_f$ . As shown in Fig. 1,  $T_f$  varies from  $T_0$  to  $T_1$  as  $H$  varies from  $(H_{el} + \Delta H_r)$  to  $H_{el}$ .

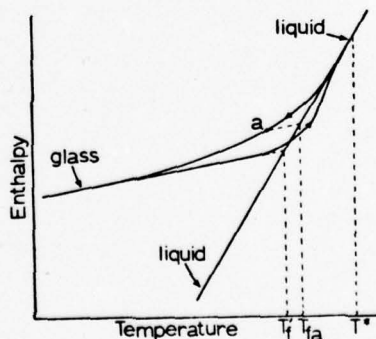


(Correspondingly, a fictive pressure  $P_f$  can be used to represent property variations during structural relaxation due to pressure changes.)

The time scale for structural relaxation of a liquid depends strongly on temperature, pressure, and structure (i.e., on  $T_f$ ). It varies from picoseconds for liquids of water-like viscosity to hours in the high viscosity annealing region of a glass.

Cooling and/or subsequent reheating of a liquid at a rate  $q$  may be thought of as a series of temperature steps  $dT$  followed by isothermal holds for time periods  $dT/q$ . Fig. 2 shows the variation of  $H$  during cooling and subsequent reheating. The change-over from liquid to glass-like behavior occurs in a temperature region (called the "glass transition region" for cooling/heating rates of  $\sim 1\text{K/min}$ ) where some characteristic time period allowed for structural proportional to  $1/q$  becomes comparable to a characteristic relaxation time  $\tau$  for the structural relaxation.

FIGURE 2. Evolution of enthalpy during cooling and subsequent heating at a constant rate.





The aim of the following publications was to arrive at an accurate empirical description of the kinetics of the variation of properties during structural relaxation, particularly in response to complicated pressure or temperature histories.

Publication No. 1

"Dependence of the Glass Transition Temperature on Heating and Cooling Rate." C.T. Moynihan, A.J. Easteal, J.A. Wilder, and J. Tucker, J. Phys. Chem., 78, 2673 (1974).

When a liquid is rate cooled or heated through the glass transition region, the onset of glass-like behavior, i.e., structural relaxation effects, is often characterized in terms of the glass transition temperature,  $T_g$ , which specifies roughly the temperature of the "break" in the property-temperature curve. For example, in Fig. 2 the temperature denoted  $T'_f$  would commonly be taken as  $T_g$ . It was known that the observed value of  $T_g$  for a glass depended on heating or cooling rate  $q$ . In this paper we showed that this interdependence of  $T_g$  and  $q$  could yield information on the kinetic parameters controlling the structural relaxation, in particular that

$$d \ln |q| / d(1/T_g) \approx -\Delta h^* / R \quad (1)$$

where  $R$  is the ideal gas constant and  $\Delta h^*$  is the activation enthalpy for the relaxation times controlling the structural relaxation. The conditions necessary for the validity of this

relation are that the structural relaxation be describable by a temperature-independent distribution of relaxation times and that the glass be cooled from a starting temperature well above the transition region and subsequently reheated at the same rate starting from a temperature well below the transition region. Experimental measurements of  $T_g$  vs.  $q$  were presented for  $As_2Se_3$ ,  $B_2O_3$ , potassium silicate, and borosilicate crown glasses.  $\Delta h^*$  was found to be equal within experimental error to the activation enthalpy for the shear viscosity.

Publication No. 2

"Dependence of the Fictive Temperature of Glass on Cooling Rate." C.T. Moynihan, A.J. Easteal and M.A. DeBolt, J. Am. Ceram. Soc., 59, 12 (1976).

It is often not possible to measure  $T_g$  over a wide range of cooling or heating rates because of lack of sensitivity of the measuring instruments at low rates and the problem of temperature gradients at high rates. In this paper it is shown that by monitoring the variation of a property during heating at a convenient experimental rate after cooling through the glass transition region at a variety of rates  $q$ , the dependence of the limiting fictive temperature  $T'_f$  attained by the glass after rate cooling can be measured. ( $T'_f$ , shown in Fig. 2, is the same as  $T_g$  defined in the most common fashion). It was shown by extending an earlier

theory of Ritland to the case of a spectrum of relaxation times that the dependence of  $T'_f$  on cooling rate  $q$  is given by

$$d \ln |q| / d(1/T'_f) \approx -\Delta h^*/R \quad (2)$$

Measurements of  $T'_f$  versus  $q$  for the property enthalpy  $H$  were carried out by differential scanning calorimetry for three glasses; typical results are shown for  $B_2O_3$  glass in Fig. 3. The  $\Delta h^*$  values assessed via Eq. (2) were in good agreement with the shear viscosity activation enthalpies in the glass transition region.

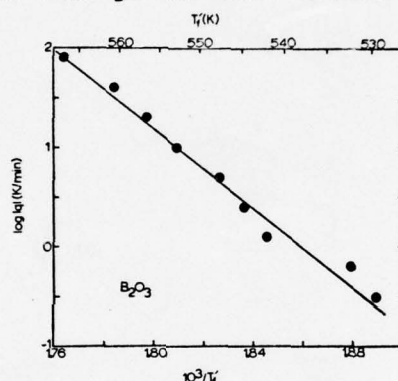


Fig. 3. Logarithm of cooling rate vs reciprocal of  $T'_f$  attained by glass after it was cooled through the transition region for  $B_2O_3$ . Points are experimental data, and solid line is plot of  $\log |q|$  vs  $10^3/T'_f$  calculated using the best-fit  $A$ ,  $\Delta h^*$ ,  $x$ , and  $\beta$  parameters.

#### Publication No. 3

"Analysis of Structural Relaxation in Glass Using Rate Heating Data." M.A. DeBolt, A.J. Easteal, P.B. Macedo and C.T. Moynihan, J. Am. Ceram. Soc. 59, 16 (1976).

This is the seminal publication in which we present our theory for the time evolution of properties of glasses due to structural relaxation in response to complicated temperature or pressure

histories, e.g., in response to a number of sequential temperature or pressure steps. The theory is cast in the form appropriate to dealing with temperature steps, but modification to allow pressure steps to be dealt with is straightforward.

In brief, we postulated that the evolution of  $T_f$  in response to a number of temperatures changes  $\Delta T_i$  applied at respective times  $t_i$  is given by the superposition principle:

$$T_f(t) = T_0 + \sum_i \Delta T_i [1 - \phi(t - t_i, t)] \quad (3)$$

where  $T_0$  is an initial equilibrium value of  $T_f$  and  $\phi$  is a non-exponential, non-linear relaxation function of the form:

$$\phi(t - t_i, t) = \sum_j g_j \exp\left(-\int_{t_i}^t dt' / \tau_j\right) \quad (4)$$

$g_j$  is a probability density function for structural relaxation times  $\tau_j$ , which depend in turn on both temperature and structure (i.e., on  $T_f$ ):

$$\tau_j = A_j \exp\left[x\Delta h^*/RT + (1 - x)\Delta h^*/RT_f\right] \quad (5)$$

where  $A_j$  and  $x$  are constants. Continuous changes in  $T$  with time (heating or cooling) can be dealt with by replacing the summation by an integral in Eq. (3).

We tested our theory by analyzing the variation in enthalpy  $H$  of  $B_2O_3$  glass during rate heating following a rate cool. In doing so we used an empirical expression for Eq. (4):



$$\phi(t - t_i, t) = \exp \left[ - \left( \int_{t_i}^t dt' / \tau \right)^\beta \right] \quad (6)$$

where  $\beta$  is a constant parameter which specifies the distribution of relaxation times,  $g_j$ , and  $\tau$  a characteristic relaxation time with a temperature and structure dependence given by Eq. (5).

The ability of our theory to account for the time dependence of  $T_f$  for a wide variety of thermal histories using a single set of kinetic parameters ( $A$ ,  $\Delta h^*$ ,  $x$ , and  $\beta$ ) is shown in Fig. 4, where we compare calculated and experimental values of  $dT_f/dT$  vs.  $T$  curves during rate heating of  $B_2O_3$ . The solid line in Fig. 3 was also predicted with this same set of parameters.

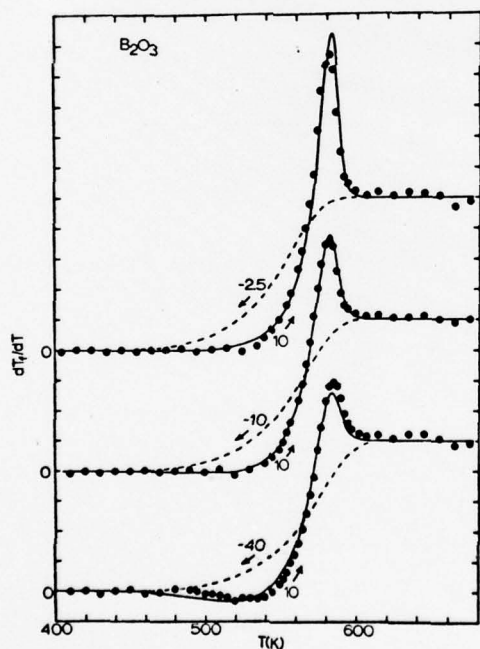


Fig. 4. Plot of  $dT_f/dT$  vs  $T$  for  $B_2O_3$  at a heating rate of 10 K/min following rate cools through transition region at rates shown (K/min) on figure. Points are experimental  $dT_f/dT$  heating curves, and solid lines are  $dT_f/dT$  heating curves calculated from the best-fit  $A$ ,  $\Delta h^*$ ,  $x$ , and  $\beta$  parameters. Dashed lines are calculated  $dT_f/dT$  cooling curves.



In this paper we also compared the relative rates of structural relaxation in  $B_2O_3$  glass measured in terms of two different properties, enthalpy  $H$  and refractive index  $n$ , and found the relative rates to be different.

Publication No. 4

"Kinetics of the Glass Transition." C.T. Moynihan, P.B. Macedo, N. Saad, M. DeBolt, B.E. Dom, A.J. Easteal and J.A. Wilder, *Fizika i Khimiya Stekla*, 1, 420 (1975).

This is the text of a paper presented at the VIth All-Union Conference on the Glassy State held in Leningrad in March, 1975. It summarized our recent work in structural relaxation, including that covered in Publications 1-3, and particularly emphasized the fact that the kinetic parameters for structural relaxation of different macroscopic properties are in general different. In support of this data were presented showing the difference in rates of relaxation during an isothermal anneal following a single temperature step of the two properties index of refraction  $n$  and logarithm of electrical conductivity,  $\ln \sigma$ , of a  $K_2O-SiO_2$  glass.

Publication No. 5

"Light Scattering Measurements of Structural Relaxation in Glass by Digital Correlation Spectroscopy." C.C. Lai, P.B. Macedo and C.J. Montrose, *J. Am. Ceram. Soc.* 58, 120 (1976).

This is the first paper applying the technique of digital correlation light scattering spectroscopy to the measurement in an oxide glass ( $0.5 \text{ Na}_2\text{O} - 0.5 \text{ K}_2\text{O} - 3 \text{ SiO}_2$ ) of linear viscoelastic relaxation. Light is scattered in the liquid from index of refraction (and hence density) fluctuations. Since these fluctuations grow and decay via the structural relaxation process, correlation analysis of the time dependence of the intensity of the scattered light at several temperatures gives the linear relaxation kinetic parameters  $A$ ,  $\Delta h^*$  and  $\beta$  (cf. Eqs. (5) and (6)) for relaxation of longitudinal strain in response to longitudinal stress. Digital correlation spectroscopy allowed measurements of relaxation on time scales in the range  $10^{-6}$  to  $10^2$  s, i.e., in the upper end of and somewhat above the glass transition region. This region is generally inaccessible by other relaxation techniques. As predicted, the temperature dependence of the longitudinal relaxation times measured by this technique agreed well with that of the shear viscosity.

Publication No. 6

"Viscoelastic Relaxation in  $\text{B}_2\text{O}_3$ ." C.C. Lai, P.B. Macêdo and C.J. Montrose, Proceedings of the Tenth International Congress on Glass, 11, 68 (1974).

In this paper the digital correlation spectroscopy technique was used to characterize linear viscoelastic relaxation in vitreous

$B_2O_3$  over an extensive temperature range. It was found that the  $\beta$  parameter, characterizing the distribution of relaxation times, was temperature dependent in regions where the shear viscosity activation enthalpy exhibited a temperature dependence. This supported models, proposed in previous papers from this laboratory, which presumed that transport in highly viscous liquids is based on cooperative motion of regions of large size.

Publication No. 7

"Structural Relaxation in Vitreous Materials." C.T. Moynihan, P.B. Macedo, C.J. Montrose, P.K. Gupta, M.A. DeBolt, J.F. Dill, B.E. Dom, P.W. Drake, A.J. Easteal, P.B. Elterman, R.P. Moeller, H. Sasabe and J.A. Wilder, Ann. N.Y. Acad. Sci., 279, 15 (1976).

This is the text of a paper presented at the Conference on the Glass Transition and the Nature of the Glassy in New York in December, 1975. It summarized our recent work in the structural relaxation. New data of interest were a comparison of the structural relaxation kinetics for enthalpy of  $As_2Se_3$  glass during rate cooling and heating and during isothermal annealing following a single temperature step and for refractive index of  $B_2O_3$  glass during isothermal annealing following one temperature step and following two temperature steps. It was shown using the analysis methods of Publication (3) that the same kinetic parameters could be used to describe the responses of the respective glasses to the

various different thermal histories. Enthalpy relaxation data and digital correlation spectroscopy results were presented for the lubricant 5P4E. A detailed comparison was made among the structural relaxation kinetic parameters for different properties (e.g.,  $V$ ,  $H$ ,  $n$ , longitudinal strain, shear stress) for a number of glasses. It was found that in general different properties of the same glass relax at different rates. It was shown using a proposed relation between the thermodynamics and kinetics of the structural relaxation via an order parameter model that this was expected from the experimental values of the heat capacity, thermal expansivity, and isothermal compressibility changes at the glass transition (i.e., from the Prigogine - Defay ratio).

Publication No. 8

"Ultrasonic Relaxation Studies in Potassium-Borate Melts."

R. Scully, J.H. Simmons and P.B. Macedo, J. Non-Cryst. Solids, 12, 18 (1973).

The  $K_2O-B_2O_3$  system, along with other alkali borate systems, shows peculiar viscosity behavior. As  $K_2O$  is added to  $B_2O_3$ , the viscosity isotherm passes first through a minimum and then through a maximum. Ultrasonic relaxation studies showed that the minimum and the maximum are due to the behavior of the most probable relaxation time and to the width of the distribution of relaxation times for longitudinal stress. These results support a model which



accounts for the viscosity on the basis of the effect of the  $K_2O$  content on the relative numbers of  $BO_3$  and  $BO_4$  groups in the melt. The ultrasonic relaxation measurements show no indication of a previously suggested phase transition in this system.



#### IV. ELECTRICAL RELAXATION AND THE MIXED ALKALI EFFECT

Ionically conducting glasses and liquids exhibit a frequency dispersion in the dielectric constant  $\epsilon'(\omega)$  and electrical conductivity  $\sigma(\omega)$  associated with the long range ionic transport, where  $\omega (= 2\pi f)$  is angular frequency. In a paper sponsored by an earlier Air Force contract (Phys. Chem. Glasses, 13, 171 (1972)) we proposed a method of analyzing this dispersion which avoided the artificial dissection of the conductivity into a d.c. component  $\sigma_0$  and an a.c. component  $(\sigma(\omega) - \sigma_0)$ , as had been done in previous treatments of this phenomenon. We suggested that attention be focused on the decay of the electric field  $E(t)$  inside the glass to zero via the long range ionic diffusion process:

$$E(t) = E(0) \phi(t) = E(0) \int_0^{\infty} g(\tau) \exp(-t/\tau) d\tau \quad (7)$$

where  $\phi(t)$  is the electric field decay function,  $\tau$  an electric field relaxation time, and  $g(\tau)$  the associated probability density function for electric field relaxation times. In the frequency domain this process could be described by an "electric modulus" or inverse complex permittivity:

$$\begin{aligned} M^*(\omega) \equiv 1/\epsilon^*(\omega) &= M_{\infty} \left[ 1 - \int_0^{\infty} dt \exp(-i\omega t) (-d\phi(t)/dt) \right] \\ &= M_{\infty} \int_0^{\infty} g(\tau) [i\omega\tau / (1 + i\omega\tau)] d\tau \end{aligned} \quad (8)$$

where  $\epsilon^*(\omega)$  is the complex permittivity:

$$\epsilon^*(\omega) = \epsilon'(\omega) - i(\sigma(\omega)/\omega\epsilon_0), \quad (9)$$

$$M_{\infty} = 1/\lim_{\omega\tau \gg 1} \epsilon'(\omega) \quad (10)$$

and  $\epsilon_0$  is the permittivity of free space. The most important feature of our formalism is that it associated the magnitude of the dispersion in  $\epsilon'(\omega)$  and  $\sigma(\omega)$  with kinetic parameters associated with the long range ionic transport, namely the distribution of relaxation times  $g(\tau)$ , rather than with thermodynamic parameters (e.g., temperature, concentration of molecular dipoles, and dipole moments), as did theories appropriate for dielectric relaxation in polar liquids and solids.

The following publications constituted, for the most part, further investigations of electrical relaxation in glass and liquid ionic conductors and application of our theory to the results.

Publication No. 9

"Decay Function for the Electric Field Relaxation in Vitreous Ionic Conductors." C.T. Moynihan, L.P. Boesch and N.L. Laberge, Phys. Chem. Glasses 14, 122 (1973).

Experimental curves for the real and imaginary parts of  $M^*(\omega)$  ( $= M'(\omega) + iM''(\omega)$ ) for ionically conducting glasses and liquids were found to be uniformly of one shape when plotted against a logarithmic frequency scale: asymmetric and skewed to higher frequencies, as shown in Fig. 5 for a 40 mol%  $\text{Ca}(\text{NO}_3)_2$  -60  $\text{KNO}_3$  melt.

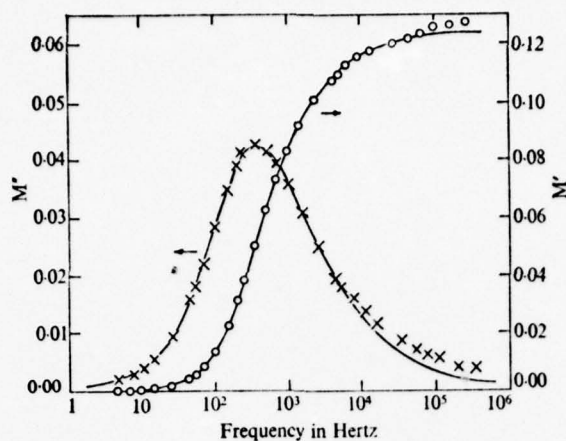


Figure 5. Experimental and calculated  $M^*(\omega)$  plots for  $0.4\text{Ca}(\text{NO}_3)_2-0.6\text{KNO}_3$  melt at  $71.4^\circ\text{C}$ .  $\beta=0.64$

x =  $M'$   
o =  $M''$

We showed that these curves could be fit well assuming an empirical electric field relaxation function

$$\phi(t) = \exp[-(t/\tau_0)^\beta] \quad (11)$$

$\beta$  ( $0 < \beta \leq 1$ ) is a parameter characterizing the distribution of relaxation times,  $g(\tau)$ , the distribution being broader the smaller the  $\beta$  value.  $\tau_0$  is a characteristic relaxation time. To obtain the calculated values of  $M^*(\omega)$  from this expression for  $\phi(t)$ , the Fourier transform of Eq. (8) must be carried out numerically on a computer. This computer calculation was done for a wide range of  $\beta$  values and tables published of values of  $M'(\omega)/M_\omega$  and  $M''(\omega)/M_\omega$  versus reduced frequency ( $\omega\tau_0$ ) for different  $\beta$  values, along with other characteristic features of the  $M'$  and  $M''$  curves (e.g., the width of the  $M''$  curves at half-height). These tables make possible the determination of the value of  $\beta$  which best describes a given set of experimental electric relaxation data.

Publication No. 10

"Electrical Relaxation in a Glass-Forming Molten Salt."

F.S. Howell, R.A. Bose, P.B. Macedo and C.T. Moynihan, J. Phys. Chem. 78, 639 (1974).

The dielectric constant  $\epsilon'$  and electrical conductivity  $\sigma$  of a glass-forming 40 mol%  $\text{Ca}(\text{NO}_3)_2$ -60 mol%  $\text{KNO}_3$  melt were measured over a frequency range of 0.02 Hz-1 MHz and a temperature range of 25-96°. Measurements were carried out both on the equilibrium liquid above 60° and the nonequilibrium glass below 60°. This was the first time a thorough set of electrical relaxation measurements had been carried out on both glass and liquid.

The observed frequency dispersions in  $\epsilon'$  and  $\sigma$  were attributed to a nonexponential decay of the electric field via the ionic diffusion process and analyzed as such. It was found that the electric field relaxation was well described by the decay function  $\phi(t) = \exp[-(t/\tau_0)^\beta]$ ,  $0 < \beta \leq 1$ . Typical results are shown in Fig. 5 for  $M'(\omega)$  and  $M''(\omega)$ .

The mean electric field relaxation time,  $\langle\tau_\sigma\rangle$ , for the liquid was found to be faster than the mean shear stress relaxation time,  $\langle\tau_s\rangle$ , by a factor ranging from 10 to  $10^4$  over the temperature range 96-60°, indicating a solid-like ionic conductivity mechanism in the highly viscous melt. The activation enthalpy for the electrical conductivity dropped from 78 kcal/mol for the equilibrium



liquid to 24 kcal/mol for the glass. The difference between liquid and glass activation enthalpies was attributed to thermally induced structural changes in the equilibrium liquid. The width of the spectrum of electric field relaxation times was temperature independent for the glass but broadened with increasing temperature for the liquid. From this it was concluded that the source of the spectrum of relaxation times was the microscopic heterogeneity of the vitreous system and that the temperature dependence of the width of the spectrum for the liquid reflected thermally induced structural changes.

Publication No. 11

"Electrical and Mechanical Relaxations in a Mixed-Alkali Silicate Glass." T.J. Higgins, L.P. Boesch, V. Volterra, C.T. Moynihan, and P.B. Macedo, J. Am. Ceram. Soc. 56, 334 (1973).

When one alkali is replaced by a second alkali in a network glass (e.g., glasses in the series  $X \text{Na}_2\text{O} - (1-X)\text{K}_2\text{O} - 3 \text{SiO}_2$  with  $0 \leq X \leq 1$ ) the ionic transport properties show striking departures from additivity. For example, the electrical conductivity at intermediate compositions passes through a minimum that may be as much as a factor  $10^6$  below the conductivity value predicted from additivity. Likewise in mixed alkali glasses there is observed a strong mechanical relaxation (relaxation of shear stress in response to applied shear strain) that is absent in the



corresponding single alkali glasses. Previous investigators found a minimum in dielectric loss at temperatures and compositions where a strong mechanical relaxation peak is observed. They concluded that the mechanism responsible for the mixed alkali mechanical relaxation peak (possibly exchange of sites between, e.g., a  $\text{Na}^+$  and a  $\text{K}^+$  ion) was electrically inactive.

We carried out an exhaustive investigation of both mechanical and electrical relaxation in a  $0.5 \text{ Na}_2\text{O} - 0.5 \text{ K}_2\text{O} - 3 \text{ SiO}_2$  glass. Our results are summarized in Fig. 6, which shows plots of the real part of the normalized mechanical modulus,  $N'$ , and of the normalized electrical modulus,  $N'_{el}$  ( $= M'(\omega)/M_\infty$ ), versus a reduced frequency  $\omega\tau_1$ . The fact that the electrical relaxation curve lies at much higher frequencies than the mechanical relaxation curve

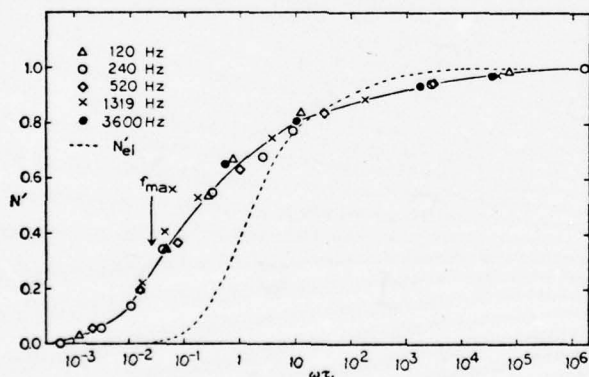


Fig. 6. Normalized relaxational part of Young's modulus,  $N'$ , vs  $\omega\tau_1$  for  $0.5\text{Na}_2\text{O}-0.5\text{K}_2\text{O}-3\text{SiO}_2$  glass;  $N'_{el}$  curve taken from Fig. 2(A) and  $f_{max}$  from Ref. 14.

means that the electric field decays much faster (perhaps via the diffusion of the more mobile cations) than does the mechanical stress field. Hence the mixed alkali mechanical peak does not

have an observed electrical analog, not because the process responsible for the mechanical relaxation is inherently electrically inactive, but rather because the driving force (the electric field) vanishes inside the glass much faster than the mixed alkali process is capable of responding to it.

Publication No. 12

"Heat Capacity and Structural Relaxation of Mixed-Alkali Glasses." C.T. Moynihan, A.J. Easteal, D.C. Tran, J.A. Wilder and E.P. Donovan, J. Am. Ceram. Soc. 59, 137 (1976).

There was some question as to whether the mixed alkali effect was confined to properties associated with ionic transport or whether mixed alkali effects could be observed in equilibrium thermodynamic properties and in dynamic properties associated with rearrangement of the network, e.g., viscosity and structural relaxation. To partially answer this question, heat capacities of a series of mixed-alkali glasses of composition (in mol%)  $24.4(\text{Na}_2\text{O} + \text{K}_2\text{O}) - 75.6 \text{ SiO}_2$  were measured in the transition region by differential scanning calorimetry. It was found that the glass heat capacities at 700 K and the equilibrium liquid heat capacities were the same for all glasses on a per-g.atom basis and equal, respectively, to  $5.6 \pm 0.1$  and  $6.8 \pm 0.1$  cal/g.atom K. The glass transition temperatures exhibited negative deviations from additivity, but the heat capacity curves in the transition region of

all the glasses for identical heating rates and thermal histories could be superimposed on the same reduced plot. This behavior indicated that the shapes of the structural relaxation functions are the same for all the glasses. These results support the conclusion that there is no unique "mixed-alkali effect" on thermodynamic or structural relaxation properties and that the term should be reserved for properties relating to ionic transport.

## V. PHASE SEPARATION AND MICROSTRUCTURE

In recent years, there has been intense activity in developing new applications of phase separated inorganic glass forming systems. These systems offer considerable potential for developing glasses with a wide range of properties. Basically there are three types of applications of phase separated glasses.

### Composite Glasses

An important example is that of glass ceramics. These are materials made from two phase glasses in which one of the phases is caused to crystallize, thus producing a glass-crystal composite. Glass ceramics have structures similar to a traditional polycrystalline ceramic, i.e., randomly oriented crystalline particles bonded together by a glass matrix but in a glass ceramic, the grain size is extremely small, about 500 Å. As yet, these materials are rather expensive and typically are used for making rocket nose cones, radomes and even some domestic ware. These still have problems in ultimate strength and too high a coefficient of expansion at high temperatures which make them fail under thermal shock. Major developments in understanding the properties of glass ceramics, however, are still limited by lack of basic research of the relation between phase separation and crystallization.

### Porous Glasses

Phase separated glasses, under certain conditions, can be made porous by leaching out preferentially one of the phases. This technique has been used in making glasses with controlled pore sizes for the isolation and purification of macromolecules and viruses. Also, with the advent of catalytic reactors to control automotive exhaust, a need has arisen for a high strength



durable and high temperature catalytic support, and porous glass has been considered as a potential candidate for such catalytic supports.

#### Reconstructed Glasses

Reconstructed glasses produced today are generally made from glasses in the alkali-borosilicate systems which are suitably heat-treated to produce a two-phase glass and subsequently leached with acid to remove one of the phases, thus forming a porous skeleton of high silica content. The high silica skeleton is then treated in a number of different ways before being heated and sintered to form a reconstructed non-porous glass. The chemical treatment prior to sintering and consolidation can be adjusted at will to develop many desired physical and chemical properties in the reconstructed glass, thus making this product versatile and easily tailored to the requirements of its application.

Most of these applications, however, are limited by the lack of basic understanding of phase separation phenomena in glasses. At Catholic University, we have over the last few years made several important contributions towards enhancing this understanding. In the following we discuss some of these problems that existed and how the research work at Catholic University helped to solve them.

The study of phase separation phenomena is generally divided into two parts, the thermodynamic and the kinetic. For simplicity, we shall limit the present discussion to systems separating into two phases only, under isothermal isobaric conditions.

A glass of average composition  $C_0$  tends to be homogeneous above the coexistence temperature (also phase boundary or binodal temperature)  $T_p(C_0)$ . After heat treatment at a temperature  $T < T_p(C_0)$

this glass separates into two phases of compositions  $C_{\alpha}^{(P)}(T)$  and  $C_{\beta}^{(P)}(T)$  (See Fig. 7).  $T_p(C)$  is therefore called immiscibility dome (coexistence curve or binodal curve). The top of the immiscibility dome defines the critical point of the system and is characterized by critical temperature  $T_c$  and critical composition  $C_c$ . At a temperature  $T < T_c$ , glass,  $C_o$  (given sufficiently long heat-treatment time) separates into two equilibrium phases,  $\alpha$  and  $\beta$ , such that the molar fraction of the minor ( $\alpha$ ) phase,  $X_{\alpha}(T, C_o)$ , is

$$X_{\alpha}(T, C_o) = \frac{C_{\beta}^{(P)}(T) - C_o}{C_{\beta}^{(P)}(T) - C_{\alpha}^{(P)}(T)}$$

The region of single phase immediately surrounding the critical point is referred to as "critical region." It is characterized by large fluctuations in composition, making the glass somewhat opalescent. These fluctuations (in the single phase region) ultimately lead to phase separation (in the two-phase region).

Unlike binary systems, the composition in a multi (three or more) component system is specified by two (or more) concentrations. Composition can therefore be thought of as a vector  $\vec{C}$ , the components of which are the individual concentrations of the independent species. In multi-component systems, the immiscibility dome extends into three (or more) dimensions. For example, for a three component glass such as  $\text{Na}_2\text{O}-\text{B}_2\text{O}_3-\text{SiO}_2$ , the immiscibility dome is three-dimensional. An isothermal section of a 3-D dome is sketched in Fig. 8. A glass of average composition  $\vec{C}_o$  separates into two phases of compositions  $\vec{C}_{\alpha}^{(P)}(T)$  and  $\vec{C}_{\beta}^{(P)}(T)$ .

The line  $\vec{C}_\alpha^{(P)}(T) - \vec{C}_\beta^{(P)}(T)$  is called "tie-line" because it joins compositions which can coexist in equilibrium. A tie-line is always a straight line, and it always passes through the average composition  $C_O$ ; furthermore, no two tie-lines can intersect. It is clear, therefore, that in the case of a multicomponent system, the immiscibility dome does not provide complete information about tie-lines.

A study of the thermodynamics of phase separation, therefore, consists in (1) plotting the immiscibility dome and (2) in the case of multi-component glasses, plotting the tie-lines.

It is possible to divide the immiscibility dome into two parts by considering the free energy-composition relationship at some temperature below  $T_C$ . A schematic plot of this relationship is shown in Fig. 9. Analysis has recently been extended to multicomponent glasses by P.K. Gupta of Catholic University.

The equilibrium compositions  $C_\alpha^{(P)}(T)$  and  $C_\beta^{(P)}(T)$  of the two phases are given by the well-known common-tangent construction.

The curvature  $\frac{\partial^2 f}{\partial C^2}$  of the free energy curve is

--positive in the region  $C_\alpha^{(P)}(T) \leq C_O < C_\alpha^{(S)}(T)$

--zero when  $C = C_\alpha^{(S)}(T)$

--negative in the region  $C_\alpha^{(S)}(T) < C_O < C_\beta^{(S)}(T)$

--zero when  $C_O = C_\beta^{(S)}(T)$

--positive in the region  $C_\beta^{(S)}(T) < C_O \leq C_\beta^{(P)}(T)$

The part of the immiscibility dome where the curvature  $\frac{\partial^2 f}{\partial C^2}$

is positive (definite) is called the "metastable region" and the part where the curvature is negative is called the "unstable region". The boundary between the metastable and unstable regions is called "spinodal curve" and is sketched in Fig. 10 schematically, along with the coexistence curve.



For an average composition  $C_0$ , the coexistence temperature  $T_p(C_0)$  is always larger or equal to the spinodal temperature  $T_s(C_0)$ . In the metastable region, phase separation occurs by a Nucleation and Growth (NG) mechanism. In the unstable region, phase separation occurs by a Spinodal Decomposition (SD) mechanism. A short comparison of the main predictions of the two theories is presented below.

In the early stages of phase-separation, SD theory, as developed by Cahn and others, predicts a preferential amplitude growth of a selected small band of Fourier components of composition fluctuations. No such preferred amplitude growth is expected for NG. Further, while NG typically gives rise to initially isolated minor phase particles (discrete morphology--only major phase connected) which may at later times coalesce, SD typically produces a connected morphology (both phases are connected over large distances).

It should be emphasized that these predictions are for the (so-called) early stages of phase separation, and coarsening in later stages is expected to produce a transition from connected to discrete morphology in the case of SD. On the other hand, in NG a connected morphology may develop by an intersecting growth mechanism starting from discrete morphology. In view of these difficulties, the morphological techniques alone cannot distinguish between NG and SD mechanisms.

Goldstein has noted that from the scattering results along it is not possible to distinguish between NG and SD. Thus an interesting question arises. Is it possible to distinguish experimentally between NG and SD? The conceptual distinction between NG and SD is in the process of nucleation, which is difficult to observe for it constitutes the very early stages of phase separation in the metastable region.



"Theoretical Analysis of Miscibility Gaps in the Alkali-Borates." P.B. Macedo and J.H. Simmons, J. Res. Nat. Bur. Stds., 78A, 53 (1974).

Interest from scientific and technological areas has long been evident in the analytical description of miscibility gaps in oxide glasses. These analytical expressions have been sought to serve both as a basis for physical modeling of phase separation thermodynamics and as a simple means for predicting phase separation temperatures for oxide mixtures with compositions of interest.

In this paper a thermodynamic approach based on regular mixing concepts was applied to modeling phase separation in alkali-borate glasses. It was found to be quite successful in describing the miscibility gap boundaries (or coexistence curve). The concept which must be introduced to accomplish this was the assumption that the glassformer phase is structurally represented by a complex molecule and the glassformer-modifier phase by a stoichiometric compound. This transformation symmetrizes the coexistence curve.

The regular mixing equation appears to represent the data well when an additional entropy of mixing arising from changes in the internal degrees of freedom of the system is included in the calculation. Following this approach, five systems were treated successfully. The complex boron trioxide molecule  $[(B_2O_3)_5]$  was used in the regular mixing analyses of all the borate systems considered, since the miscibility gaps occurred approximately within the same temperature range.

The implications of such an approach are interesting but not surprising. As mentioned before, by other authors and in some of our other work, the existence of complex glass-former structures

in the melt appears to offer a good explanation for the behavior of an increasing number of physical properties of molten oxide glasses.

An actual gemoetrical description of the complex boron trioxide structure was not possible by this analysis since thermodynamic treatments do not afford structural descriptions.

Publication No. 14

"On the Determination of Spinodal Temperature by Electron Microscopy." A. Sarkar, P.K. Gupta, G.R. Srinivasan, V. Volterra and P.B. Macedo, J. Chem. Phys. 59, 4246 (1973).

Composition fluctuations present in the supercritical region (the single phase region near the critical point of an immiscibility dome) of a multicomponent glass can be observed by replica electron microscopy provided (1) it is possible to quench these (composition) fluctuations to room temperature through a large two phase region and (2) an etching agent is available which is sufficiently sensitive to expose small compositional variations. We were also able to study the isothermal growth of such fluctuations in the supercritical region of a sodium borosilicate glass having a small amount of alumina. The main effect of alumina is to lower the immiscibility dome and thereby bring the supercritical region in a high viscosity domain.

Of particular interest in these studies is the temperature dependence of the equilibrium fluctuation size,  $\ell(T, C_0)$ . [ $\ell(T, C_0)$  is the mean intercept length of a micrograph of a sample of average composition,  $C_0$ , which has been heat treated at a temperature,  $T$ , for long time.] These results are closely approximated by a power law

$$\ell(T, C_0) = K[T - T_0(C_0)]^{-\nu} \quad (1)$$

with three independent parameters:  $K$ ,  $\nu$  and  $T_0$ . For the two glasses studied:

(i) the exponent,  $\nu$ , seems to be the same for both glasses and is about  $0.5 \pm 0.005$ ,

(ii) the constant,  $K$ , also appears to be the same in both glasses and is about  $743 \pm 20 [\text{\AA} (\text{°C})^{1/2}]$ ,

(iii) the constant,  $T_0$ , however is significantly different for the two glasses; i.e.,  $T_0 = T_0(C_0)$ .

For the glass without alumina  $T_0$  is about 753.5 ( $^{\circ}\text{C}$ ) and for the glass with alumina  $T_0$  is about  $649 \pm 0.5(^{\circ}\text{C})$ . We note that for both glasses, the values of  $T_0$  found are less than the respective coexistence temperatures,  $T_p(C_0)$ .

In our preliminary efforts to explain these results, we suggested that the measured  $\ell(T, C_0)$  is some temperature dependent characteristic length of the system and may be related to the correlation length,  $\xi(T, C_0)$ . The classical theories predict, for critical composition  $C_c$ ,

$$\xi(T, C_c) \approx (T - T_c)^{-\nu} \quad \nu = 0.50. \quad (2)$$

A reasonable extension of Eq. (2) to noncritical compositions is obtained by substituting for  $T_c$  in Eq. (2) the (so-called spinodal) temperature  $T_{sp}(C_0)$ , i.e.,

$$\xi(T, C_0) \approx [T - T_{sp}(C_0)]^{-0.50} \quad (3)$$

[The spinodal temperature for a noncritical composition,  $C$ , defines the lower limit of metastability of a homogeneous system in the two phase region. For such a system, the Helmholtz free energy density  $f(T, C)$ , should be analytic in the entire  $T$ - $C$  plane (including the critical point and the coexistence curve), and

$$\partial^2 f / \partial C^2 |_{C_0, T_{sp}(C_0)} = 0.]$$

Owing to the remarkable agreement of the values of exponent  $\nu$  for the observed data [Eq. (1)] and classical theories [Eq. (3)], we assumed that

$$\ell(T, C_0) = \text{const.} \cdot \xi(T, C_0) \quad (4)$$

where the proportionality constant in Eq. (4) is temperature independent. Equation (4) implies that



$$T_o(C_o) = T_{Sp}(C_o). \quad (5)$$

The purpose of this paper was to report an examination of the validity of Eq. (5). For this purpose we obtained an independent estimate of  $T_{Sp}(C_o)$  from equilibrium measurements in the two phase region. In particular, we measured the volume fraction of the minor phase at various temperatures in the two phase region. Our results agree with Eq. (5).

Publication No. 15

"Analysis of Composition Fluctuation Lifetimes in a critical Oxide Mixture by Volume Relaxation Spectroscopy." J.H. Simmons and P.B. Macedo, J. Non-Cryst. Solids 11, 357 (1973).

The propagation of sound waves near the critical point can be used to examine the effect of composition fluctuations on the diffusion coefficient.

Longitudinal and shear ultrasonic measurements were conducted above the phase transition temperature of a soda borosilicate glass mixture. The distribution of volume relaxation times in the mixture was calculated from longitudinal and shear modulus measurements. The ultrasonic relaxation measurements allowed the investigation of two distinct effects in the distribution of relaxation times as the temperature was lowered toward the critical point. At high temperatures, a coupling between the compressional component of the ultrasonic wave and supercritical fluctuations in composition was observed as an anomalous broadening of the distribution of volume relaxation times. This interaction allowed a measure of the average composition fluctuation lifetime,  $\tau_D$ , as a function of temperature. At lower temperatures, as  $\tau_D$  became longer than the volume relaxation times, the behavior of the distribution followed closely the predictions of an environmental relaxation model proposed by these authors for the analysis of shear relaxation processes in the same material.

Publication No. 16

"Small Angle X-ray Scattering Study of Spinodal Decomposition in the  $B_2O_3$ -PbO- $Al_2O_3$  System." G.R. Srinivasan, R. Colella, P.B. Macedo, and V. Volterra, Phys. Chem. Glasses, 14, 90 (1973).

The theoretical basis to our understanding of spinodal decomposition has largely come from the work of Hillert, Cahn, and Hilliard in the past decade. Notable improvement to this early development has been made recently by Cook, who considered the effect of random thermal fluctuations (analogous to Brownian motion) on the spinodal kinetics. His theory provides an explanation for the experimentally observed curvature in the  $R(\vec{k})/k^2$  plot for two component systems, where  $R(\vec{k})$  is the growth rate of composition fluctuation with wave vector  $\vec{k}$  and  $k = |\vec{k}|$ . However, Cook's theory predicts a common crossover point for all small-angle x-ray scattering (SAXS) curves which represent the early stages of the decomposition including the initial, "as quenched" state. A survey of the published SAXS data from various systems shows that the curves from as quenched samples do not intersect those corresponding to early stages of spinodal decomposition at this common point. This raises the question whether or not the occurrence of the crossover point is a necessary feature of the linear spinodal theory.

We demonstrate from theoretical considerations that occurrence of a cross-over point (i.e., the critical wave vector for which the growth rate is zero) represents the onset of nonlinear stages in the spinodal growth, provided the initial conditions are such that prior decomposition has not occurred at some lower temperature. This conclusion was verified in a SAXS experiment on the  $B_2O_3$ -PbO- $Al_2O_3$ .

Publication No. 17

"Electron Microscope Observations of Phase Separation near Spinodal Boundary in a Sodium Borosilicate Glass." G.R. Srinivasan, A. Sarkar, P.K. Gupta, and P.B. Macedo, J. Non-Cryst. Solids, 20, 141 (1976).

In recent years several studies have attempted to distinguish between two commonly accepted mechanisms of phase separation in glasses, namely nucleation and growth (N&G) and spinodal decomposition (SD). The studies using light or small angle x-ray scattering can directly verify Cahn's spinodal decomposition theory which predicts the preferential growth of a selected band of Fourier components of the composition fluctuations in the scattering spectra. The prediction for N&G mechanism is quite different, in that no such selective growth is expected. Electron-microscope studies are based on the notion that while the N&G process produces initially isolated minor phase particles distributed randomly in the matrix phase (assuming no foreign surfaces exist in the melt), the SD produces an interconnected morphology in which both phases are connected over large distances in the sample. It is emphasized that these predictions are for early stages of the phase separation, and coarsening in later stages is expected to produce a break in the interconnectivity of the spinodal microstructure. On the other hand, interconnectivity in N&G microstructure can result by an intersecting growth mechanism as proposed by Haller. In view of these difficulties, the morphological method of distinguishing between the N&G and SD mechanism remains controversial.

We studied volume fraction of the minor phase in an alumina doped sodium borosilicate glass inside the immiscible region. It was shown that such a study permits a distinction between the two



mechanisms of phase separation, namely spinodal decomposition and nucleation and growth. For spinodal decomposition, the volume fraction decreases initially, whereas for nucleation and growth it increases with heat-treatment time.

Publication No. 18

"Effect of Subcritical Microstructure on the Viscosity of a Sodium Borosilicate Glass." R. Mahoney, G.R. Srinivasan, P.B. Macedo, A. Napolitano and J.H. Simmons, *Phys. Chem. Glasses*, 15, 24 (1974).

Critical point theories have generally predicted that the diffusion coefficient vanishes at the transition temperature. Near the transition temperature of oxide glasses, we have observed large but finite increases in viscosity which are related to inverse of the diffusion coefficient. However, far below the transition temperature "anomalous" viscosity behavior should be expected due to the two-phase nature of the glass.

In this paper viscosity and electron microscopy measurements were reported on a phase separating glass as a function of time, at various temperatures. The viscosity changed by five orders of magnitude during the phase separation in a time period identified to be solely in the coarsening stage by electron microscopy. The stage during which composition changes are dominant occurs very quickly despite the high starting viscosity ( $10^{11}$  P) and, therefore, is nearly complete before reliable viscosity data can be obtained (2 min). Analysis of the rate of increase of the average particle size identified a rearrangement stage proceeding by bulk diffusion through the fluid phase with an apparent activation energy of 98 k/cal mole ( $4.1 \times 10^5$  J/mole). Superposition of the viscosity-microstructure size curves for various temperatures demonstrated that the change in viscosity was totally controlled by the growth of the viscous phase whose activation energy for viscosity is 132 k/cal mole ( $5.52 \times 10^5$  J/mole). The change of viscosity with time

was explained in terms of changes in the size of the micro-structure by applying an environmental relaxation model proposed by two of the authors.